

Confined Growth of Cyanide-Based Magnets in Two Dimensions

Eugenio Coronado,* Carlos Martí-Gastaldo, Efrén Navarro-Moratalla, and Antonio Ribera

Universidad de Valencia (ICMol), Polígono de la Coma s/n, 46980 Paterna, Spain

Received December 21, 2009

Herein we report the first hybrid magnetic material resulting from the intercalation of a cyanide-based molecular magnet into a solid-state layered host. More specifically, the use of a diamagnetic cationic $\text{Zn}^{\text{II}}\text{--Al}^{\text{III}}$ layered double hydroxide host allows for the formation of an anionic two-dimensional ferromagnetic $\text{Ni}^{\text{II}}\text{--Cr}^{\text{III}}$ Prussian Blue analogue, from the templated assembly of its ionic molecular components in the confined interlamellar space offered by the inorganic host.

Molecule-based materials have shown to be particularly significant in materials science because they provide a fruitful source of multifunctional materials.¹ In particular, the hybrid approach, in which two or more different molecular building blocks are combined, has been extremely rewarding in the design of new materials exhibiting an unusual mixing of physical properties.² A variation of this approach relies on the combination of molecule-based components with solid-state inorganic structures, yielding hybrid materials that combine the robustness of the inorganic host with the flexibility of molecular building blocks. So far, this strategy has permitted the organization and confinement of functional molecules at the nanoscale, finding particular interest in optical and magnetic properties.³ Here we propose the use of layered double hydroxides (LDHs) to template the formation of extended two-dimensional (2D) layers of bimetallic cyanide-bridged coordination polymers (CPs). Although this strategy has been recently exploited to insert polynuclear bimetallic oxalato complexes into a diamagnetic $\text{Mg}^{\text{II}}\text{--Al}^{\text{III}}$ LDH,⁴ the poor matching between the density charges of

both ionic sublattices prevented polymerization of these complexes in the interlamellar space.⁵ In fact, the charge density of the $[\text{M}^{\text{II}}\text{M}^{\text{III}}(\text{ox})_3]^-$ anionic layer is significantly smaller than that of the LDH cationic layers: -0.013 and $+0.028 \text{ q}\cdot\text{Å}^{-2}$, respectively. To overcome this problem, we decided to survey the formation of an anionic 2D lattice based on the cyanide ligand (CN^-), whose smaller size in comparison with the oxalate could help to properly fit the density charge imposed by the positively charged LDH layers (-0.024 compared to $+0.028 \text{ q}\cdot\text{Å}^{-2}$). A second reason that justifies this choice resides in the ability of CN^- to transmit magnetic interactions and generate a wide diversity of magnetic materials,⁶ including room temperature magnets⁷ and photoinduced⁸ or pressure-induced⁹ switchable magnets. Finally, from a synthetic point of view, this could be an excellent opportunity to check whether the confined growth of a three-dimensional (3D) Prussian Blue analogue (PBA) lattice from its ionic components in the interlamellar space provided by the LDH host might stabilize an anionic 2D PBA, still nonexistent.

As the LDH host, we chose $[\text{Zn}_2\text{Al}(\text{OH})_6]^+$, which is diamagnetic, and as the bimetallic cyanide guest, the derivative $[\text{NiCr}(\text{CN})_6]^-$, which in bulk behaves as a ferromagnet with $T_C = 90 \text{ K}$.¹⁰ The nitrate salt of the ZnAl LDH (**1**) was prepared in good yield as a polycrystalline pure phase according to the coprecipitation route proposed by Miyata.¹¹ The nitrate exchange was carried out by immersing the pristine LDH- NO_3 material in a saturated aqueous solution of $\text{K}_3[\text{Cr}(\text{CN})_6]$. The resulting white powder, ZnAl- $[\text{Cr}(\text{CN})_6]$ LDH (**2**), was collected by filtration in almost quantitative yield. In a second step, **2** was suspended

*To whom correspondence should be addressed. E-mail: eugenio.coronado@uv.es.

(1) (a) Miller, J. S. *Adv. Mater.* **1990**, *2*, 98–99. (b) Awaga, K.; Coronado, E.; Drillon, M. *MRS Bull.* **2000**, *25*, 52–57.

(2) (a) Coronado, E.; Galán-Mascarós, J. R.; Gómez-García, C. J.; Laukhin, V. *Nature* **2000**, *408*, 447–449. (b) Coronado, E.; Day, P. *Chem. Rev.* **2004**, *104*, 5419–5448. (c) Bénard, S.; Yu, P.; Audié, J. P.; Rivière, E.; Clément, R.; Ghilhem, J.; Tchertanov, L.; Nakatani, K. *J. Am. Chem. Soc.* **2000**, *122*, 9444–9454.

(3) Vo, V.; Minh, N. V.; Lee, H. I.; Kim, J. M.; Kim, Y.; Kim, S. J. *Mater. Res. Bull.* **2008**, *44*, 78–81.

(4) Coronado, E.; Galán-Mascarós, J. R.; Martí-Gastaldo, C.; Ribera, A. *Chem. Mater.* **2006**, *18*, 6112–6114.

(5) Preliminary results indicate that formation of an extended CP of $\text{Mn}^{\text{II}}\text{--Cr}^{\text{III}}\text{--ox}$, exhibiting spontaneous magnetization at low temperatures, is feasible through the more versatile exfoliation/restacking approach instead of the ionic-exchange method.

(6) Shatruck, M.; Avendano, C.; Dunbar, K. R. *Progress in Inorganic Chemistry*; Karlin, K. D., Ed.; Wiley-VCH: Weinheim, Germany, 2009; Vol. 56, Chapter 3, pp 155–334.

(7) (a) Ferlay, S.; Mallah, T.; Ouahès, R.; Veillet, P.; Verdager, M. *Nature* **1995**, *378*, 701–703. (b) Holmes, S. M.; Girolami, S. G. *J. Am. Chem. Soc.* **1999**, *121*, 5593–5594.

(8) Sato, O.; Iyoda, T.; Fujishima, A.; Hashimoto, K. *Science* **1996**, *272*, 704–705.

(9) (a) Bleuzen, A.; Lomenech, C.; Escax, V.; Villain, F.; Varret, F.; Cartier, C.; Verdager, M. *J. Am. Chem. Soc.* **2000**, *122*, 6648–6652. (b) Coronado, E.; Giménez-López, M. C.; Korzeniak, T.; Levchenko, G.; Romero, F. M.; Segura, A.; García-Baonza, V.; Cezar, J. C.; de Groot, F. M. F.; Milner, A.; Paz-Pasternak, M. *J. Am. Chem. Soc.* **2008**, *130*, 15519–15532.

(10) Gadet, V.; Mallah, T.; Castro, I.; Verdager, M. *J. Am. Chem. Soc.* **1992**, *114*, 9213–9214.

(11) (a) Miyata, S. *Clays Clay Miner.* **1980**, *28*, 50–56; **1980**, *19*, 591–596. (b) Miyata, S.; Okada, A. *Clays Clay Miner.* **1977**, *25*, 14–18.

in a 1:1 (v/v) mixture of methanol/ethylene glycol containing an excess of $\text{NiNO}_3 \cdot 6\text{H}_2\text{O}$. Polymerization of the ionic components in the restrained 2D space offered by the inorganic host resulted in the formation of $\text{ZnAl}[\text{Cr}^{\text{III}}\text{Ni}^{\text{II}}(\text{CN})_6(\text{NO}_3)_2]$ LDH (**3**), which was collected as a yellowish solid (see SI 1 in the Supporting Information for experimental details). Note that, in order to balance the charge, in the resulting cyanide bimetallic layer two of the CN^- anions of the PBA have been substituted with two NO_3^- anions, which are probably occupying the axial positions of the octahedral Ni site. The metallic composition, as estimated from an energy-dispersive analysis of X-rays (EDAX; see SI 3 in the Supporting Information), indicates that the Zn/Al ratio remains almost constant for **1–3**, thus discarding any chemical change affecting the brucite-like sheets during the intercalation/polymerization processes. The Cr/Zn ratio equal to 0.12 in **2** indicates that the $[\text{Cr}(\text{CN})_6]^{3-}$ intercalation proceeds in good yield (AEC estimated around 70%). Deviation with respect to complete exchange must be ascribed to the co-intercalation of carbonate (vide infra). This ratio remains constant in **3** after Ni^{2+} intercalation, while the Ni/Cr ratio, 1.15, suggests the formation of a cyanide-linked $\text{Cr}^{\text{III}}\text{–Ni}^{\text{II}}$ network, in good agreement with that expected for the ideal value of the $\text{Ni}^{\text{II}}/\text{Cr}^{\text{III}} = 1$ CP.

Fourier transform infrared (FT-IR) was employed to check the presence of residual nitrate and carbonate anions (the latter representing the main source of contamination in the synthetic route) and monitor the nature of the intercalated moieties in each case (see SI 4 in the Supporting Information). The water content was estimated from thermogravimetric analysis (see SI 5 in the Supporting Information). The presence of $[\text{Cr}(\text{CN})_6]^{3-}$ in **2** is confirmed by the vibration mode in the cyanide triple-bond stretching region ($2100\text{--}2200\text{ cm}^{-1}$). Peak shifts or fine structure alterations in comparison with the simple $\text{K}_3[\text{Cr}(\text{CN})_6]$ salt must be ascribed to host–guest chemical interactions and a preferential orientation of the metallic complex in the LDH interlamellar space.¹² The formation of coordination bonds in **3** is supported by variation in the wavelength of the cyanide vibration modes and a change in its multiplicity. The homogeneity of the resulting sample and the absence of a contaminant 3D PBA phase, resulting from a combination of the ionic components from the LDH host, were confirmed by means of scanning electron microscopy (SEM; see SI 6 in the Supporting Information).

Figure 1 shows the powder X-ray diffraction data for **1–3**. They exhibit the typical LDH pattern with sharp well-defined peaks at low θ values, while they become broader and less defined at higher angular values. This indicates that the crystallinity of the pristine material is maintained in the intercalated compounds. Assuming rhombohedral $3R$ symmetry, low θ peaks can be indexed as $(00l)$ reflections, thus permitting the estimation of the unit cell parameters in each case (Table 1). From these values, augmentation of the basal spacing (BS) from 8.8 Å in **1** up to 11.2–11.1 Å in **2** and **3** is observed. This fact is unambiguously provoked by the substitution of NO_3^- anions with the metallic complex. The difference between the van der Waals width of the brucite-like sheets, ca. 4.7 Å, and the estimated BSs permits the calculation of gallery heights of 4.1 Å for **1** and 6.5–6.4 Å

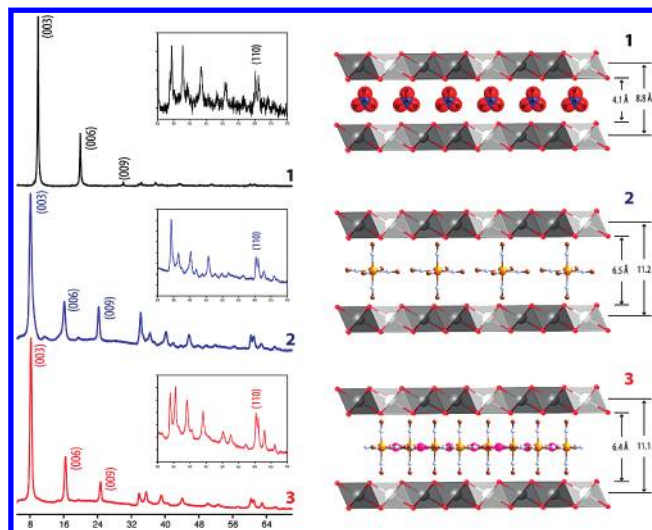


Figure 1. Powder X-ray diffraction patterns (left) and schematic representation of the parent and intercalated materials (right).

Table 1. Powder X-ray Diffraction Data and Calculated Parameters of **1–3**

	(hkl)				calcd param [Å] ^a		
	(003)	(006)	(009)	(110)	a	c	BS
1	9.95	19.95	30.10	60.20	2.9	26.5	8.8
2	8.15	15.70	23.60	60.15	3.1	33.4	11.2
3	8.03	15.90	23.87	60.33	3.1	33.3	11.1

$$^a a = 2d_{110}; c = (d_{003} + 2d_{006} + 3d_{009}); \text{BS} = c/3.$$

for **2** and **3**, respectively. These values are in good agreement with those previously reported¹³ and suggest that $[\text{Cr}(\text{CN})_6]^{3-}$ complexes orientate their C_4 axes perpendicularly to the LDH layers. Note that this preferential orientation might promote a differentiation of the cyanide ligands into two groups: axial, strongly attached to the $-\text{OH}$ -covered LDH layers by means of hydrogen-bonding interactions, and equatorial, more likely to interact with metallic ions in the subsequent polymerization step. In this way, the inorganic host will act as a templating agent, preventing the formation of a 3D polymeric PBA system and restricting its growth in two dimensions. This point seems to be confirmed by the gallery height calculated for **3**, which remains almost constant after the divalent metal loading and subsequent formation of the bimetallic 2D CP.

Magnetic susceptibility measurements of **2** were carried out with an applied field of 1000 G in the 2–300 K range. As is expected for a paramagnetic system, χ_M follows an exponential regime in the whole temperature range (see SI 7 in the Supporting Information) with an estimated value for the Curie constant, $C = 0.50\text{ emu} \cdot \text{mol}^{-1}$, in excellent agreement with the value calculated for the chromium content derived from the metallic analysis, $0.45\text{ emu} \cdot \text{mol}^{-1}$. The paramagnetic behavior of **2** is additionally supported by the fitting of the isothermal field dependence of magnetization to the Brillouin function ($S_{\text{Cr}^{\text{III}}} = 1.5$; see SI 7 in the Supporting Information). The estimated $g = 1.8$ value slightly deviates from that expected for an isotropic Cr^{III} ion, probably as a

(12) Carpani, I.; Berrettoni, M.; Giorgetti, M.; Tonelli, D. *J. Phys. Chem. B* **2006**, *110*, 7265–7269.

(13) (a) Holgado, M. J.; Rives, V.; Sanromán, M. S.; Malet, P. *Solid State Ionics* **1996**, *92*, 273–283. (b) Hansen, C. B. H.; Koch, B. C. *Clays Clay Miner.* **1994**, *42*, 170–179.

Communication

result of the presence of dipolar interactions in the LDH interlayer space.

Upon cooling, the $\chi_M T$ product of **3** remains almost constant from its room temperature value of $0.85 \text{ emu} \cdot \text{mol}^{-1}$ (expected value: $0.82 \text{ emu} \cdot \text{mol}^{-1}$) down to 100 K (Figure 2a); then, it starts to increase abruptly, suggesting the presence of ferromagnetic Cr^{3+} – Ni^{2+} coupling through the cyanide bridge, as is expected from the strict orthogonality between the magnetic orbitals t_{2g} and e_g .¹⁴ The positive $\theta = +71.4 \text{ K}$ extracted from the fitting of the magnetic susceptibility to the Curie–Weiss law additionally supports this point (see SI 9 in the Supporting Information). $M(H)$ measured at 2 K shows the typical profile for a soft ferromagnet (Figure 2a, inset), with a fast increase of the magnetization up to 0.15 T, reaching saturation at higher fields ($M_S = 1.1 \mu_B$ at 5.5 T; expected value $M_S = 1.3 \mu_B$) and a small coercive field of 0.14 kG (see SI 10 in the Supporting Information).

The presence of a long-range magnetic ordering in **3** was confirmed with dynamic magnetic measurements, explored in the 1–10 000 Hz interval with an external applied field of 3.95 G. Both the in-phase (χ_M') and out-of-phase (χ_M'') components of the alternating-current (ac) susceptibility define a peak below 70 K (Figure 2b). A minor frequency dependence of the maximum position is observed for χ_M'' . This feature is probably related to the dynamics of the domain walls in the frozen ferromagnetic state, as was previously observed for other bimetallic cyanide-bridged 2D ferromagnets.¹⁵ Attending to the temperature for which the χ_M'' signal becomes positive, the cyanide-based bimetallic CP formed in the LDH interlamellar space exhibits ferromagnetic ordering at ca. 65 K. This value is approximately four-sixths of that reported for the classical 3D Ni^{II} – Cr^{III} PBA ($T_C = 90 \text{ K}$).¹⁰ Given that in a general approximation T_C is proportional to the number of effective magnetic neighbors (N),¹⁶ this decrease seems to indicate that while in the 3D PBA case each Cr center is surrounded by six Ni atoms ($N = 6$), only four effective magnetic interactions are present in **3** ($N = 4$). Therefore, the LDH host has played an effective templating role in **3**, forcing the $[\text{Cr}(\text{CN})_6]^{3-}$ and Ni^{II} ionic components to interconnect in two dimensions.

In summary, we have reported here the first example describing the intercalation of a molecule-based magnet into a solid-state host. In this case, the use of a cationic LDH host templates the formation of an anionic 2D cyanide-based bimetallic molecular ferromagnet from the directed assembly of its molecular components in the confined interlamellar space offered by the LDH, preventing formation of the thermodynamically favored 3D system. Notice that so far the methods employed for reducing the dimensionality of the bimetallic cyanides were based on the use of capping ligands or on the growth of monolayers onto substrates by means of the Langmuir–Blodgett technique.¹⁷ In comparison with

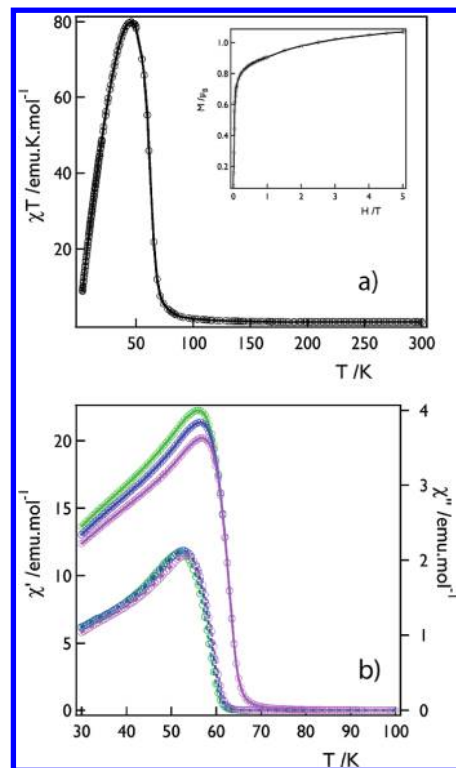


Figure 2. (a) Thermal dependence of the $\chi_M T$ product of **3** in the 2–300 K interval. Inset: field dependence of the magnetization at 2 K. (b) ac susceptibility of **3** at 100 (green), 1000 (blue), and 10000 Hz (lavender). In-phase and out-of-phase susceptibilities are represented by filled and empty symbols, respectively.

these methods, our approach is solely based in inorganic building blocks. It provides an efficient way to design more complex inorganic/inorganic magnetic hybrids in which the physical properties of the molecule-based magnets, including the photomagnetism exhibited by the PBAs, are expected to be combined with, or even coupled to, those introduced by the employment of magnetic LDHs.¹⁸

Acknowledgment. Financial support from the EU (MolSpinQIP and Advanced Grant ERC SPINMOL), the Spanish Ministerio de Ciencia e Innovación (MICINN; Project Consolider-Ingenio in Molecular Nanoscience and projects MAT2007-61584 and CTQ-2008-06720), and the Generalitat Valenciana (Prometeo Program) is gratefully acknowledged. E.N.-M. thanks the MICINN for a predoctoral grant. We also acknowledge F. M. Romero for helpful scientific discussions and J. M. Martínez-Agudo for his help with the magnetic measurements.

Supporting Information Available: Details concerning the synthesis, physical characterization, EDAX analysis, SEM images, FT-IR study, thermogravimetric analysis, and additional magnetic characterization of the compounds reported herein. This material is available free of charge via the Internet at <http://pubs.acs.org>.

(14) Pei, Y.; Journaux, Y.; Kahn, O. *Inorg. Chem.* **1989**, *28*, 100–103.

(15) Coronado, E.; Gómez-García, C. J.; Nuez, A.; Romero, F. M.; Waerenborgh, J. C. *Chem. Mater.* **2006**, *18*, 2670–2681.

(16) (a) Verdaguier, M.; Bleuzen, A.; Marvaud, V.; Vaissermann, J.; Seuleiman, M.; Desplanches, C.; Sculler, A.; Train, C.; Garde, R.; Gelly, G.; Lomenech, C.; Rosenman, I.; Veillet, P.; Cartier, C.; Villain, F. *Coord. Chem. Rev.* **1999**, *190*, 1023–1047. (b) Néel, L. *Ann. Phys. Paris* **1948**, *3*, 137–198.

(17) (a) Lescouëzec, R.; Toma, L.; Vaissermann, J.; Verdaguier, M.; Delgado, F. S.; Ruiz-Pérez, C.; Lloret, F.; Julve, M. *Coord. Chem. Rev.* **2005**, *249*, 2691–2729. (b) Culp, J. T.; Park, J.-H.; Frye, F.; Huh, Y.-D.; Meisel, M. W.; Talham, D. R. *Coord. Chem. Rev.* **2005**, *249*, 2642–2648.

(18) (a) Laget, V.; Hornick, C.; Rabu, P.; Drillon, M.; Ziessel, R. *Coord. Chem. Rev.* **1998**, *178–180*, 1533–1553. (b) Coronado, E.; Galán-Mascarós, J. R.; Martí-Gastaldo, C.; Ribera, A.; Palacios, E.; Castro, M.; Burriel, R. *Inorg. Chem.* **2008**, *47*, 9103–9110. (c) Almansa, J. J.; Coronado, E.; Martí-Gastaldo, C.; Ribera, A. *Eur. J. Inorg. Chem.* **2008**, 5642–5648.